Effect of Position Isomerism on the Formation and Physicochemical Properties of Pharmaceutical Co-Crystals

XIANGMIN LIAO,[1] MOHAN GAUTAM,[2] ANDREAS GRILL,[1] HAIJIAN JIM ZHU[1]

[1]Forest Laboratories, Inc., 49 Mall Drive, Commack, New York 11725

[2]University of Chicago, Chicago, Illinois 60637

Received 9 January 2009; revised 17 April 2009; accepted 20 April 2009

Published online 5 June 2009 in Wiley InterScience (www.interscience.wiley.com). DOI 10.1002/jps.21824

ABSTRACT: The effect of position isomerism on the co-crystals formation and physicochemical properties was evaluated. Piracetam was used as the model compound. Six position isomers, 2,3-, 2,4-, 2,5-, 2,6-, 3,4-, and 3,5-dihydroxybenzoic acid (DHBA), were used as the co-crystal formers. Co-crystals were prepared on a 1:1 molar ratio by crystallization from acetonitrile. The solid-state properties of co-crystals were characterized using X-ray powder diffractometry (XRD), differential scanning calorimetry (DSC), and Fourier transform infrared (FTIR). All co-crystal formers formed co-crystal with piracetam except 2,6-DHBA. This failure was possibly due to steric hindrance of two bulk hydroxyl groups and preference of intra-molecular hydrogen bonding formation between hydroxyl group and carboxylic acid group. The XRD patterns of resulting co-crystal indicated that they are highly crystalline and different than parental compounds. Based on the single crystal data, P_23DHBA is orthorhombic while P_24DHBA, P_34DHBA, and P_35DHB belong to monoclinlic system. The hydrogen bonding network patterns of the co-crystals are also different. DSC data showed that the melting temperatures of resulting co-crystals are all lower than that of the starting materials. The melting point rank order of the co-crystals is: P_24DHBA > P_34DHBA > P_23DHBA > P_25DHBA > P_35DHBA. © 2009 Wiley-Liss, Inc. and the American Pharmacists Association J Pharm Sci 99:246–254, 2010

Keywords: co-crystal; position isomer; piracetam; dihydroxybenzoic acid

INTRODUCTION

Pharmaceutical co-crystals represent a class of compound in which an active pharmaceutical ingredient (API) complexes with one or more molecules (co-crystallizing agents) in the crystal lattice through noncovalent bonding.[1] Recently, pharmaceutical co-crystals are attracting a great deal of attention due to their desirable chemical, physical and biopharmaceutical properties. Numerous reports showed the successful improvement of properties, such as solubility, dissolution rate, physical stability and mechanical properties,[2–7] through the utilization of co-crystal concept. As a result, much like salt and polymorph screenings, co-crystal screening has become a routine preformulation process, in the pharmaceutical research development world. Although the benefit of improved API properties makes co-crystal forms a rewarding endeavor, the associated labor-intensive and time-consuming screening process is a constraint. Therefore, a better understanding of the mechanism behind co-crystal formation is essential.

Co-crystals design has been exploited by crystal engineering strategy and is based on the understanding of molecular interactions between

Correspondence to: Xiangmin Liao (Telephone: 631-858-5066; Fax: 631-858-5955; E-mail: xiangmin.liao@frx.com)

Journal of Pharmaceutical Sciences, Vol. 99, 246–254 (2010)

functional groups, especially hydrogen bonding interactions. The current practice is to first evaluate the possibility of forming supramolecular synthons between API and co-crystal formers, such as the carboxylic acid–amide, carboxylic acid–pyridine, amide–amide, and alcohol–amide synthons. A Cambridge Structural Database (CSD) survey can usually provide a rationale for coformer selection process. However, co-crystallization is a complex molecular recognition event that can be influenced by many factors, including geometry, functional group position and steric hindrance. Consequently, it is difficult and at times erroneous to predict the possibility of co-crystal formation using chemical structure solely as the basis. A recent finding[8] showed that even for highly analogous compounds with similar molecular structures, skeletons, and functional groups, co-crystals formed with different guests molecules.

The aim of this study was to evaluate the effect of position isomerism of co-crystal formers on the formation and subsequent physicochemical properties of co-crystals. Due to its structural simplicity, piracetam was chosen as the model compound in the present study. Piracetam (2-oxo-1-pyrrolidine acetamide) is a nootropic drug that enhances cognition and memory, and improves Alzheimer's and dementia.[9] As shown in Figure 1, it is a small molecule with an amide functional group. Recently, co-crystals of piracetam with benzoic acid and 2,5-dihydroxybenzoic acid (gentisic acid) were reported.[10] Six dihydroxybenzoic acids (shown in Fig. 1) were selected as co-crystal formers. The desired supramolecular synthon was a carboxylic acid–amide and it was expected that all six dihydroxybenzoic would form co-crystals based on a molecular interaction analysis.

Co-crystal preparation was attempted by crystallization from solution evaporation. Co-crystals were characterized by single crystal XRD, powder XRD, DSC, and FTIR. Elucidation of single crystal data was not provided here since it was not the focus in this study.

EXPERIMENTAL

Materials

Piracetam and 2,5-dihydroxybenzoic acid (25DHBA, 98%) were purchased from MP Biomedicals, Inc. (Solon, OH). 2,3-Dihydroxybenzoic acid (23DHBA, 99%), 3,4-dihydroxybenzoic acid (34DHBA, 98%), 3,5-dihydroxybenzoic acid (35DHBA, 97%), and 2,6-dihydroxybenzoic acid (26DHBA, 98%) were obtained from Sigma–Aldrich, Inc. (St. Louis, MO). 2,4-Dihydroxybenzoic acid (24DHBA, 98%) was purchased from Fluka, Inc. (Buchs, Germany). All materials were used as received without further purification. The corresponding co-crystals were

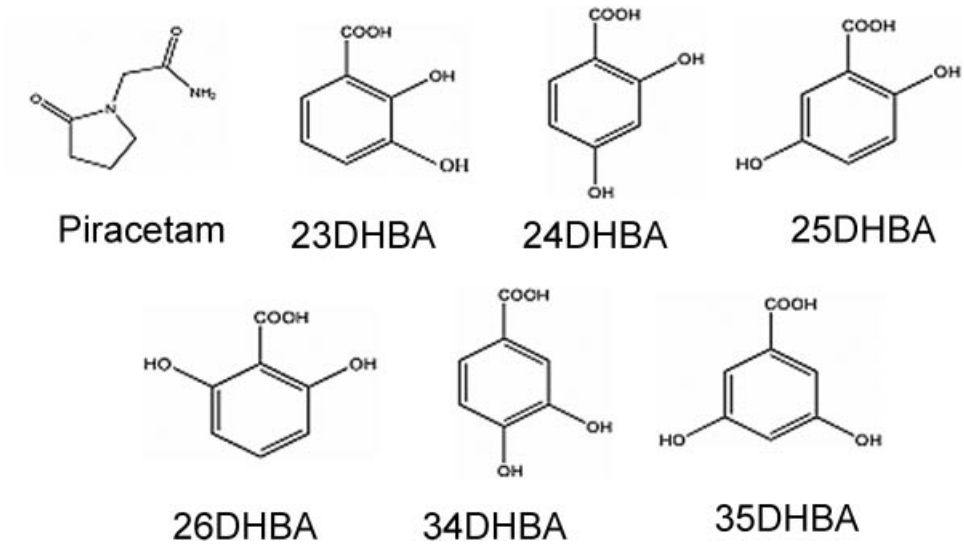

Figure 1. Chemical structure of piracetam, 2,3-dihydroxybenzoic acid (23DHBA), 2,4-dihydroxybenzoic acid (24DHBA), 2,5-dihydroxybenzoic acid (25DHBA), 2,6-dihydroxybenzoic acid (26DHBA), 3,4-dihydroxybenzoic acid (34DHBA)and 3,5-dihydroxybenzoic acid (35DHBA).

abbreviated as P_23DHBA, P_24DHBA, P_25DHBA, P_34DHBA, and P_35DHBA, respectively.

Preparation of Co-Crystals

A 1:1 mixture of piracetam (142.0 mg, 1 mmol) and co-crystal formers (1 mmol) was added to 10–15 mL of acetonitrile in a 20 mL vial. The solution was then evaporated in a hood. A crystal suitable for single crystal XRD analysis was obtained through slow evaporation over a week.

X-Ray Powder Diffractometry (XRD)

The powder XRD experiments were performed on a Rigaku miniflex X-ray diffractometer (Danvers, MA). The sample was placed on a zero background holder and exposed to Cu Kα radiation (30 kV × 15 mA). The angular range was 2–40° 2θ, and counts were accumulated at a continuous scan rate of 1°/min. The data analysis program used was JADE 8.0.

Differential Scanning Calorimetry (DSC)

A differential scanning calorimeter (MDSC, Model Q1000, TA Instruments, Wilmington, DE) with a refrigerated cooling accessory was used. The DSC cell was calibrated using indium.

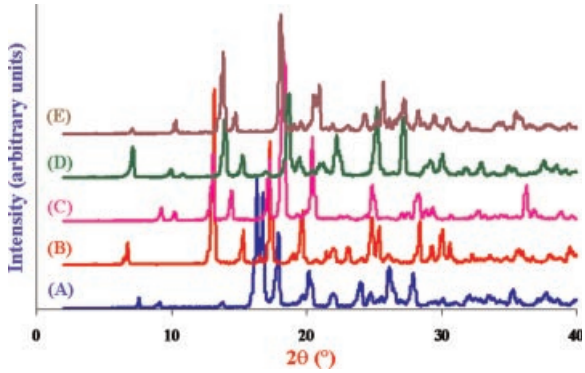

Figure 2. Overlaid XRD patterns of (A) piracetam—2,3-dihydroxybenzoic acid, (B) piracetam—2,4-dihydroxybenzoic acid, (C) piracetam—2,5-dihydroxybenzoic acid, (D) piracetam—3,4-dihydroxybenzoic acid, and (E) piracetam—3,5-dihydroxybenzoic acid.

Approximately 3–8 mg of co-crystal was weighed in an aluminum pan, sealed hermertically, and heated from 25 to 300°C at 10°C/min heating rate under nitrogen flow.

Attenuated Total Reflectance Fourier Transform Infrared Spectroscopy (ATR-FTIR)

A Thermo-Nicolet Nexus-670 unit equipped with a DTGS detector (Thermo Instrument Co.,

Table 1. Crystallographic Data of Co-Crystals

Compounds	P_23DHBA	P_24DHBA	P_25DHBA*	P_34DHBA	P_35DHBA
Empirical formula	$C_{13}H_{16}N_2O_6$	$C_{13}H_{16}N_2O_6$	$C_{13}H_{16}N_2O_6$	$C_{13}H_{16}N_2O_6$	$C_{13}H_{16}N_2O_6$
Formula weight 296.28	296.28	296.28	296.28	296.28	296.28
Crystal system	Orthorhombic	Monoclinic	Monoclinic	Monoclinic	Monoclinic
Space group	$P2_12_12$	$C2/c$	$C2/c$	$P2_1/n$	$P2_1/n$
a (Å)	10.8745(9)	27.596(4)	27.896(3)	14.3510(12)	14.7824(14)
b (Å)	24.235(2)	5.4611(9)	5.1762(5)	5.7003(5)	5.1242(5)
c (Å)	5.1710(4)	18.300(3)	19.7879(18)	17.5002	18.5139
≅ (°)	90	90	90	90	90
≅ (°)	90	98.049(3)	101.090(2)	110.371(1)	106.875(1)
≅ (°)	90	90	90	90	90
Volume (Å^3)	1362.76(19)	2730.8(8)	2803.9(4)	1342.07(19)	1342.0(2)
Z	4	8	8	4	4
Density (g/cm^3)	1.444	1.441	1.404	1.4661.466	
ABS coefficient (mm^{-1})	0.116	0.115	0.112	0.117	0.117
Reflections collected	16,134	9760	7622	11,050	15,455
Independent reflections	1848	3088	2873	3030	3043
Observed reflections	1670	2213	2417	2366	2564
$R1$ [$I > 2 \cong (I)$]	0.0309	0.0494	0.043	0.0381	0.0351
$wR2$ (all data)	0.0822	0.1048	0.108	0.0906	0.0949
Goodness-of-fit on $F2$ $wR2$ (all data)	1.068	1.05		1.012	1.095

*data excerpted from reference 10.

Madison, WI) was used for all spectra acquisition. Samples were placed under a zinc selenide (ZnSe) attenuated total reflectance (ATR) crystal accessory and a torque of ~20 cN m was applied to ensure full contact. Two hundred coadded scans were collected at a resolution of 2 cm^{-1} within the region of 4000–600 cm^{-1}.

Single Crystal X-Ray Powder Diffractometry

A single crystal was placed onto the tip of a 0.1 mm diameter glass capillary and mounted on a CCD area detector diffractometer for a data collection at 173(2) K. A preliminary set of cell constants was calculated from reflections harvested from three sets of 20 frames. These initial sets of frames were oriented such that orthogonal wedges of reciprocal space were surveyed. This produced initial orientation matrices determined from 59 reflections. The data collection was carried out using Mo Kα radiation (graphite monochromator) with a frame time of 10 s and a detector distance of 4.9 cm. A randomly oriented region of reciprocal space was surveyed to the extent of one sphere and

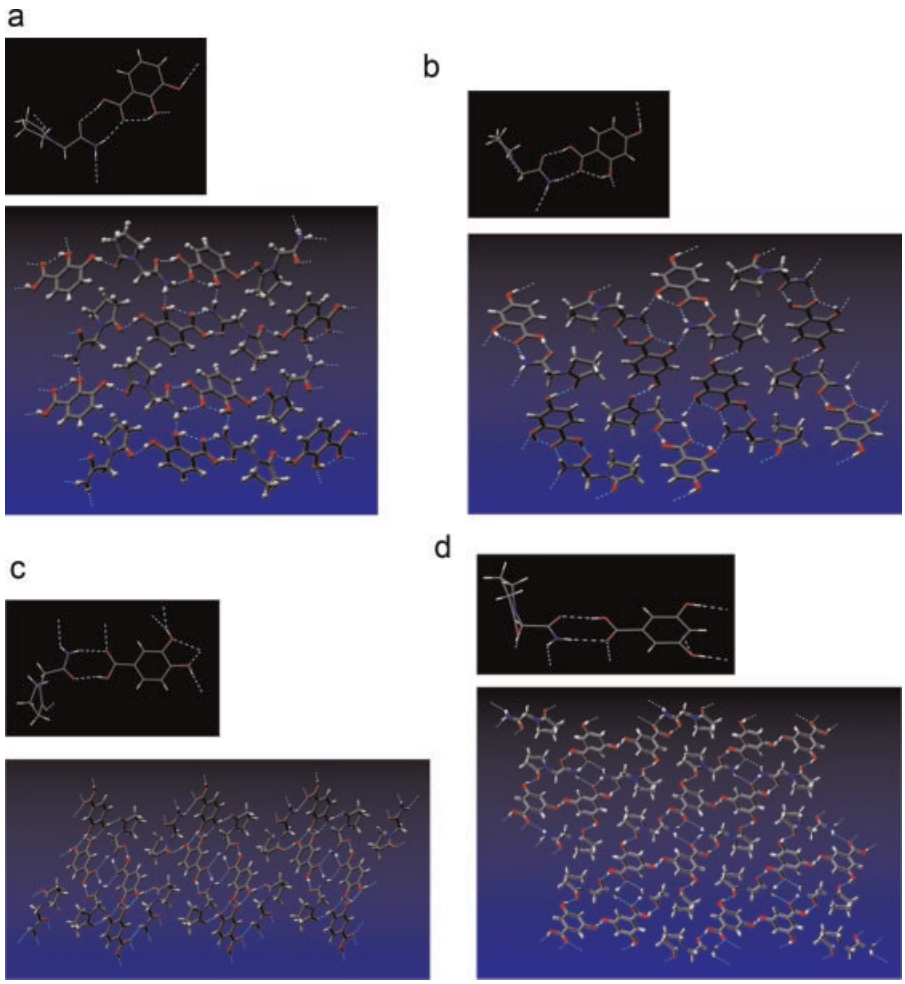

Figure 3. (**a**, **top**) The carboxylic acid—amide heterosynthon in the 1:1 co-crystal of piracetam and 23DHBA. (**Bottom**) A portion of the hydrogen bond next work in the 1:1 co-crystal of piracetam and 23DHBA. (**b**, **top**) The carboxylic acid–amide heterosynthon in the 1:1 co-crystal of piracetam and 24DHBA. (**Bottom**) A portion of the hydrogen bond next work in the 1:1 co-crystal of piracetam and 24DHBA. (**c**, **top**) The carboxylic acid–amide heterosynthon in the 1:1 co-crystal of piracetam and 34DHBA. (**Bottom**) A portion of the hydrogen bond next work in the 1:1 co-crystal of piracetam and 34DHBA. (**d**, **top**) The carboxylic acid–amide heterosynthon in the 1:1 co-crystal of piracetam and 35DHBA. (**Bottom**) A portion of the hydrogen bond next work in the 1:1 co-crystal of piracetam and 35DHBA.

to a resolution of 0.77 Å. Four major sections of frames were collected with 0.30° steps in ω at four different ϕ settings and a detector position of −28° in 2θ. The intensity data were corrected for absorption and decay. Final cell constants were calculated from the actual data collection after integration.

RESULTS AND DSICUSSION

All co-crystal formers formed co-crystals with piracetam except the 26DHBA. The powder XRD patterns of co-crystals displayed sharp diffraction peaks with high intensity and a flat baseline (Fig. 2). The co-crystals all exhibited unique patterns which are distinguished from both piracetam and their corresponding co-crystal formers. The structure of each co-crystal was determined by single crystal X-ray diffraction. A summary of crystallographic data are displayed in Table 1. PXRD patterns of the co-crystals also matched well with the simulated patterns derived from single crystal structure. Close examination of crystallographic data shows that only P_23DHBA belongs to orthorhombic system while the remaining co-crystals are monoclinic. Moreover, among monoclinic systems, P_24DHBA and P_25DHBA belong to $C2/c$ space group while P_34-DHBA and P_35DHBA are in $P2_1/n$ space group. However, the hydrogen bonding network is the focus of analysis in this study. It is evident from Figure 3 hydrogen bonds formed between carboxylic acid and amide moieties in all co-crystals. For P_23DHBA, P_24DHBA and P_25DHBA, the 2-hydroxy group not only forms an intramolecular hydrogen bond with the carbonyl group of the carboxylic acid, but also acts an acceptor to the anti-oriented NH of the primary amide. The other hydroxyl group, either in the 3, 4, or 5 position, serves as a donor to the ring carbonyl of piracetam. AS to P_34DHBA and P_35DHBA, there is no intramolecular hydrogen bond due to the lack of 2-hydroxy group. The anti-oriented NH of the primary amide connects with

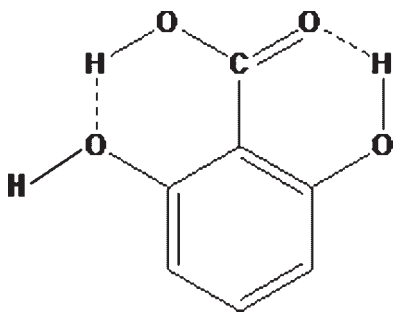

Figure 4. Proposed intermolecular hydrogen bonding formation of 26DHBA.

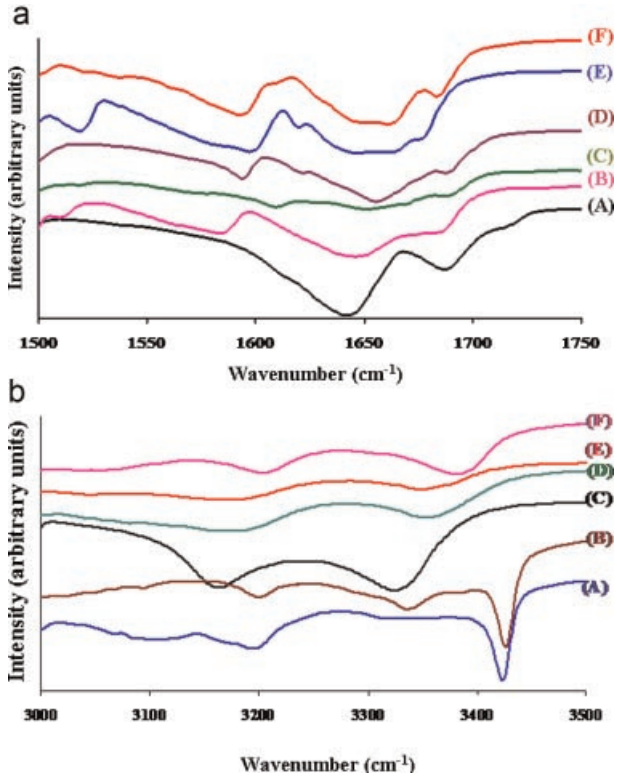

Figure 5. (**a**) FTIR spectra of (A) piracetam, (B) P_23DHBA, (C) P_24DHBA, (D) P_25DHBA, (E) P_34DHBA, and (F) P_35DHBA between 1500 and 1750 cm^{-1} region. (**b**) FTIR spectra of (A) P_35DHBA, (B) P_34 DHBA, (C) piracetam, (D) P_25DHBA, (E) P_24DHBA, and (F) P_23DHBA between 3000 and 3500 cm^{-1} region.

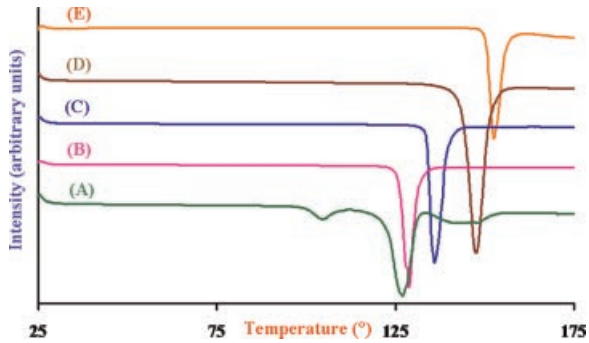

Figure 6. Overlaid DSC profiles of (A) P_35DHBA, (B) P_25DHBA, (C) P_23DHBA, (D) P_34DHBA, and (E) P_24DHBA.

the carbonyl of the carboxylic acid of another DHBA, thus forming a tetramer. Between P_34DHBA and P_35DHBA, some differences exist in how the hydroxyl groups connect. In P_35DHBA, one hydroxyl group binds to the ring carbonyl of piracetam while the other interacts with one hydroxyl group from another 35DHBA molecule. As for P_34DHBA, 3-hydroxy group acts as the hydrogen bond donor to both the 3- and 4-hydroxy group of another 34DHBA molecule while the 4-hydroxy group donates hydrogen to the ring carbonyl of piracetam. Based on the above structural analysis, 26DHBA co-crystal formation may be inhibited by two factors: First, both 2- and 6-hydroxy groups have a steric hindrance on the approach of piracetam. This steric effect was observed in several studies.[11,12] Second, both the 2- and 6-hydroxy groups may form an intramolecular hydrogen bond with 1-carboxylic acid group (Fig. 4). This reduces intermolecular hydrogen bonding ability,[11] thus eliminate the chance of carboxylic acid–amide synthon formation.

Infrared spectroscopy is a very sensitive tool used to detect molecular interactions. It has been used to monitor the secondary structure of peptides,[13] hydrogen bonding structures[14] and others.[15] N–H stretching bands is extremely sensitive in terms of both position and intensity to changes in hydrogen bonding structures.[15] As mentioned in the previous XRD analysis, hydrogen bonds are formed between amide (CO–NH) and carboxylic acid (COOH) groups. Therefore, it is expected that the vibration frequency of CO and NH will be affected by the formation of hydrogen bonds. Bands between 1500 and 1750 cm^{-1}(mainly CO group stretching mode) of co-crystals and piracetam are shown in Figure 5a. The bands at 1690 and 1640 cm^{-1} of piracetam correspond to the symmetric and anti-symmetric C=O stretching modes, respectively. In the co-crystals, the band at 1640 cm^{-1} shifted to higher wavenumbers. Since C=O stretching mode of ionized carboxylic acids are below 1600 cm^{-1}, this suggests the presence of un-ionized carboxylic acids and thus new co-crystal phases. In addition, an analysis of hydrogen bonding data confirmed that the distance between acid proton and the O atom of the carboxylic acid was constant at 0.88 Å for all co-crystals (Tab. 3). In the 3000–3500 cm^{-1} N–H stretching band region, piracetam showed two bands, at 3165 and 3330 cm^{-1}, which were assigned to intermolecular hydrogen bonded N–H to C–O. A small shift in both bands is observed in the FTIR spectra of all co-crystals. This shift is caused by the change from the hydrogen bond between two piracetam molecules to the hydrogen bond between one piracetam molecule and one dihydroxybenzoic acid molecule. However, there is a peak at approximately 3430 cm^{-1} in P_34DHBA and P_35DHBA but not in the other samples. This high frequency band is assigned to the O–H stretching frequency of hydroxyl groups.

Table 2. Melting Point of Starting Materials and Corresponding Co-Crystals

Starting Materials	Melting Point (°C)	Co-Crystals	Melting Point (°C)
Piracetam	152.1		
2,3-DHBA	207.7	P_2,3-DHBA	133.9
2,4-DHBA	224.8	P_2,4-DHBA	150.5
2,5-DHBA	201	P_2,5-DHBA	126.1
2,6-DHBA	172.6		
3,4-DHBA	201.4	P_3,4-DHBA	144.1
3,5-DHBA	237.9	P_3,5-DHBA	120.6

Table 3. Selected Hydrogen Bond Parameters of Co-Crystals

Co-Crystals	D–H···A	d(D–H)/Å	d(H···A)/Å	d(D···A)/Å	θ(D–H···A)/°
P_23DHBA	N2–H2C···O3	0.88	2.08	2.933(2)	163
	O4–H4C···O2	0.84	1.74	2.5595(19)	165.4
P_24DHBA	N2–H2A···O3	0.88	2.06	2.914(2)	163.9
	O4–H4A···O2	0.84	1.76	2.5810(18)	166.3
P_34DHBA	N2–H2A···O3	0.88	2.12	2.9731(16)	162.2
	N2–H2B···O3#3	0.88	2.29	2.9946(15)	137.2
	O4–H4C···O2	0.84	1.76	2.5859(15)	165.1
P_35DHBA	N2–H2C···O3	0.88	2.07	2.9233(14)	163.5
	N2–H2D···O3#1	0.88	2.22	2.9256(14)	136.8
	O4–H4C···O2	0.84	1.78	2.6103(12)	168.9

Thermo behavior of the resulting co-crystals was also characterized by DSC, as shown in Figure 6. All samples displayed a sharp melting endotherm, indicating highly crystalline materials. For P_35DHBA, the first endotherm (~105°C) could possibly be due to polymorphic transition and the last endotherm (~140°C) could be decomposition after melting. The meting points of co-crystals and starting materials are tabulated in Table 2. Their melting points of the co-crystals

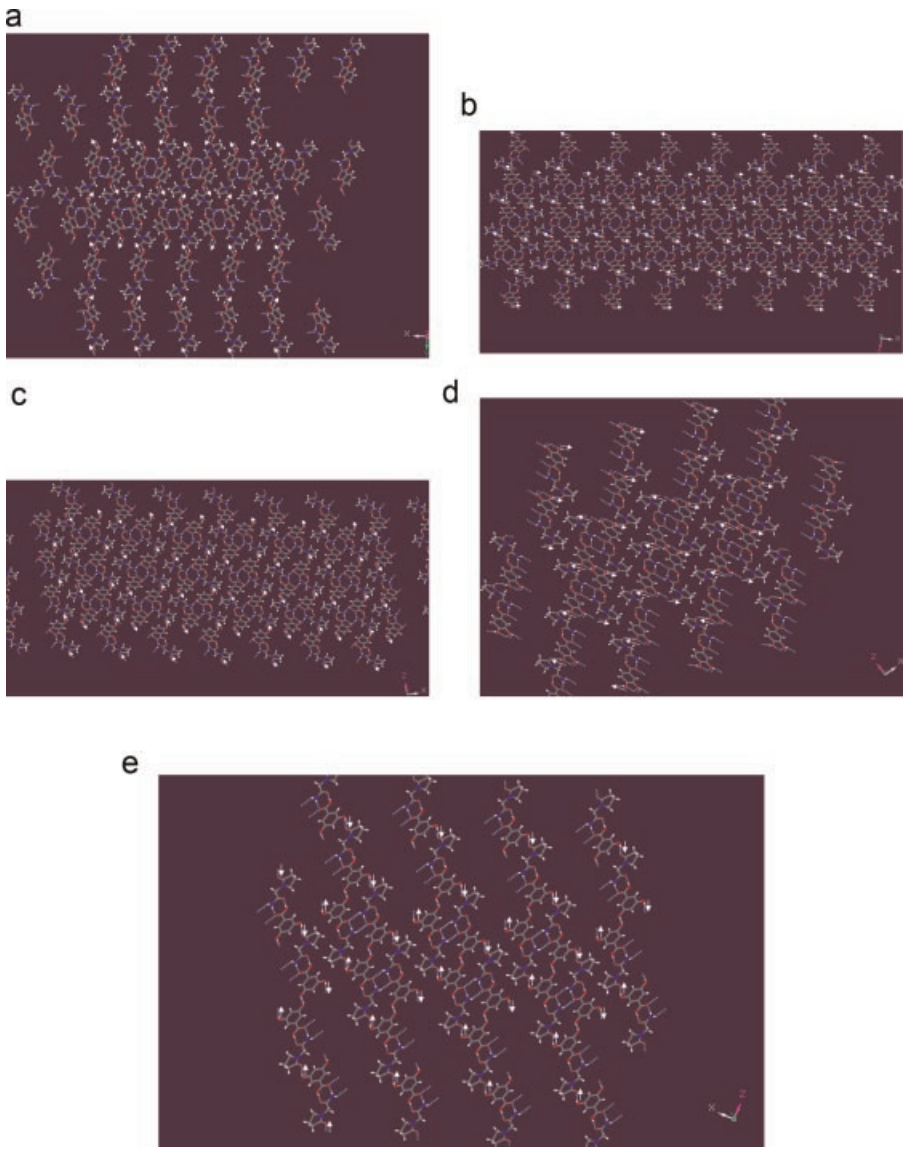

Figure 7. (**a**) Hydrogen bonding network patterns in the 1:1 co-crystal of piracetam and 2,3-dihydroxybenzoic acid. The arrows show the direction of hydrogen bond from the donor to the acceptor. (**b**) Hydrogen bonding network patterns in the 1:1 co-crystal of piracetam and 2,4-dihydroxybenzoic acid. The arrows show the direction of hydrogen bond from the donor to the acceptor. (**c**) Hydrogen bonding network patterns in the 1:1 co-crystal of piracetam and 2,5-dihydroxybenzoic acid. The arrows show the direction of hydrogen bond from the donor to the acceptor. (**d**) Hydrogen bonding network patterns in the 1:1 co-crystal of piracetam and 3,4-dihydroxybenzoic acid. The arrows show the direction of hydrogen bond from the donor to the acceptor. (**e**) Hydrogen bonding network patterns in the 1:1 co-crystal of piracetam and 3,5-dihydroxybenzoic acid. The arrows show the direction of hydrogen bond from the donor to the acceptor.

range from 120 to 150°C although all co-crystals are position isomers. The melting point of co-crystals was all lower than that of starting materials. The rank order of melting point for co-crystals was: P_24DHBA > P_34DHBA > P_23DHBA > P_25DHBA > P_35DHBA, while the rank order of dihydroxybenzoic acids was: 35DHBA > 24DHBA > 23DHBA > 34DHBA ≥ 25DHBA. Generally, there is a correlation between melting point and density. Higher density means the molecules pack closer in the crystal lattice and thus leads to higher melting point. However, a few anomalies are noted that P_24DHBA has the second lowest density but the highest melting point. Further, P_35DHBA has the highest density but the lowest melting point. While P_34DHBA has the same density as P_35DHBA, it has the second highest melting temperature. When closely examining the hydrogen bonding network of all co-crystals, some difference between them are observed. Here the focus is the hydrogen bond linking the co-crystal molecular (the arrows pointed in Fig. 7). As shown in Figure 7b and d, P_24DHBA and P_34DHBA adopt a regular double chain-antiparallel formation while P_23DHBA, P_25DHBA, and P_ 35DHBA show a regular double chain-parallel formation. According to a recent study,[16] the strength of antiparallel formation is higher than that of parallel formation, which may explain both P_24DHBA and P_34DHBA have a higher melting point. However, it is difficult to build a quantitatively correlation between melting point and structure since many factors, such as hydrogen bonding strength and numbers of hydrogen bonding, have to be taken into consideration. As demonstrated by this study, the unexpected large variation in melting point (30°C) underscores the complexity in correlation between structure and prediction of chemical and physical properties. On the other hand, modification of melting point by co-crystallization may provide additional pharmaceutical processing pathways, such as melt crystallization and hot melt extrusion, without compromising the chemical stability of API.

CONCLUSIONS

Position of function groups has indeed a significant impact not only on the formation of co-crystals, but also on the physicochemical properties of the subsequent co-crystals. Change of positions also causes different hydrogen bonding network patterns, which affects the melting point. Therefore, position isomerism should be taken into consideration in designing co-crystals with desirable properties.

ACKNOWLEDGMENTS

The authors would like to thank Dr. Raj Suryanarayanan (University of Minnesota), Dr. Ritesh Sanghvi (Forest Laboratories, Inc.), and Leanne Grafmuller (University of Pennsylvania) for reviewing the manuscript. Dr. Victor G. Young, Jr. is acknowledged for providing single crystal X-ray diffraction data.

REFERENCES

1. Vishweshwar P, McMahon JA, Bis JA, Zaworotko MJ. 2006. Pharmaceutical co-crystals. J Pharm Sci 95:499–516.
2. Fleischman SG, Kuduva SS, McMahon JA, Moulton B, Bailey Walsh RD, Rodriguez-Hornedo N, Zaworotko MJ. 2003. Crystal engineering of the composition of pharmaceutical phases: Multiple-component crystalline solids involving carbamazepine. Cryst Growth Des 3:909–919.
3. Remenar JF, Morissette SL, Peterson ML, Moulton B, MacPhee JM, Guzman HR, Almarsson O. 2003. Crystal engineering of novel cocrystals of a triazole drug with 1,4-dicarboxylic acids. J Am Chem Soc 125:8456–8457.
4. Trask AV, Motherwell WDS, Jones W. 2005. Pharmaceutical cocrystallization: Engineering a remedy for caffeine hydration. Cryst Growth Des 5:1013–1021.
5. Trask AV, Motherwell WDS, Jones W. 2006. Physical stability enhancement of theophylline via cocrystallization. Int J Pharm 320:114–123.
6. McNamara DP, Childs SL, Giordano J, Iarriccio A, Cassidy J, Shet MS, Mannion R, O'Donnell E, Park A. 2006. Use of a glutaric acid cocrystal to improve oral bioavailability of a low solubility API. Pharm Res 23:1888–1897.
7. Sun CC, Hou H. 2008. Improving mechanical properties of caffeine and methyl gallate crystals by cocrystallization. Cryst Growth Des 8:1575–1579.
8. Takata N, Shiraki K, Takano R, Hayashi Y, Terada K. 2008. Cocrystal screening of stanolone and mestanolone using slurry crystallization. Cryst Growth Des 8:3032–3037.
9. Winblad B. 2005. Piracetam: A review of pharmacological properties and clinical uses. CNS Drug Rev 11:169–182.

10. Vishweshwar P, McMahon JA, Peterson ML, Hickey MB, Shattock TR, Zaworotko MJ. 2005. Crystal engineering of pharmaceutical co-crystals from polymorphic active pharmaceutical ingredients. Chem Commun 4601–4603.
11. Abraham MH, Dearden JC, Bresnen GM. 2006. Hydrogen bonding, steric effects and thermodynamics of partitioning. J Phys Org Chem 19:242–248.
12. Dearden JC, Bresnen GM. 2005. Thermodynamics of water-octanol and water-cyclohexane partitioning of some aromatic compounds. Int J Mol Sci 6:119–129.
13. Rozenberg M, Shoham G. 2007. FTIR spectra of solid poly-L-lysine in the stretching NH mode range. Biophys Chem 125:166–171.
14. Dalterio R, Huang XS, Yu K-L. 2007. Infrared and nuclear magnetic resonance spectroscopic study of secondary amide hydrogen bonding in benzoyl PABA derivatives (retinoids). Appl Spectrosc 61: 603–607.
15. Iogansen AV. 1999. Direct proportionality of the hydrogen bonding energy and the intensification of the stretching n(XH) vibration in infrared spectra. Spectrochim Acta Part A 55A:1585–1612.
16. Simperler A, Watt SW, Bonnet PA, Jones W, Motherwell WDS. 2006. Correlation of melting point of inositols with hydrogen bonding patterns. CrystEngComm 8:589–600.